J Sol-Gel Sci Techn (2007) 42:287–292
DOI 10.1007/s10971-007-0741-9

Sol-gel processing of lead-free (Na,K)NbO_3 ferroelectric films

Fengping Lai · Jing-Feng Li

Published online: 27 February 2007
© Springer Science + Business Media, LLC 2007

Abstract The sol-gel processing of lead-free (Na,K) NbO_3 ferroelectric films was studied. Sodium ethoxide ($NaOC_2H_5$) and potassium ethoxide (KOC_2H_5) were prepared by reacting solid Na and K with ethanol (99.7%) in a solvent of 2-methoxyethanol. 0.5-μm-thick (Na,K)NbO_3 thin films with orthorhombic perovskite structure were obtained by pyrolyzing at 400°C and annealing at 800–900°C. The films had relatively dense and uniform microstructure with grain size of about 50 nm, whose ferroelectricity was proved by the *P-E* hysteresis loop measurement. It was found that excess K was effective to reduce the annealing temperature for the crystallization of sol-gel-derived (Na,K)NbO_3 thin films.

Keywords Sol-gel process · Lead-free piezoelectric ceramic · Ferroelectric · Thin film · $NaNbO_3$-$KNbO_3$

1 Introduction

As a lead-free ferroelectric and piezoelectric ceramic, $NaNbO_3$-$KNbO_3$ system has received increasing attention because it is more environmentally friendly than other lead-free piezoelectric ceramics as Bi-based lead-free ceramics [1–5]. Recent studies have been devoted to the fabrication process of (Na,K)NbO_3-based bulk materials and the enhancement of their piezoelectric and ferroelectric properties through microstructural and compositional controlling [6–8]. Compared with bulk materials, ferroelectric and piezoelectric films are important for memory and microsensor as well as microactuator applications in micro-electromechanical systems (MEMS) [9, 10]. In addition, studies on films may provide possibility for us to deeply understand the intrinsic properties of the corresponding materials, because it is possible to grow textured or epitaxial films to control their crystallographic orientations [11].

(Na,K)NbO_3-based films have been prepared by various physical and chemical methods, such as high vacuum rf-magnetron sputtering [12], pulsed laser deposition (PLD) [13], metalorganic chemical vapor deposition (MOCVD) [14] and sol-gel method [15]. The sol-gel process has obtained particular interest because of its chemical homogeneity and easiness of stoichiometry control. A further advantage of sol-gel routes is the simplicity. The similarities between sol-gel method and processing of photoresist layers also make implementation in a microfabrication facility possible. So far, we have successfully prepared textured and epitaxial Pb(Zr,Ti)O_3-based thin films on silicon and oxide single crystal wafers using the sol-gel process [11, 16].

In this work, the synthesis of lead-free $Na_{0.5}K_{0.5}NbO_3$ (abbreviated as NKN hereafter) ferroelectric films by a modified sol-gel process was studied with an emphasis on the investigation of process parameters that affect the quantity of the deposited films. 0.5-μm-thick films were prepared on silicon wafer substrates and its microstructure and ferroelectricity were characterized.

2 Experimental

Figure 1 shows the flow char of the procedure for preparing the NKN films by the sol-gel process. A starting solution was prepared by reacting 0.001 mol solid Na and 0.001 mol solid K with 3 ml ethanol (99.7%) in a solvent of

F. Lai · J.-F. Li (✉)
State Key Laboratory of New Ceramics and Fine Processing, Department of Materials Science and Engineering, Tsinghua University, Beijing 100084, P. R. China
e-mail: jingfeng@mail.tsinghua.edu.cn

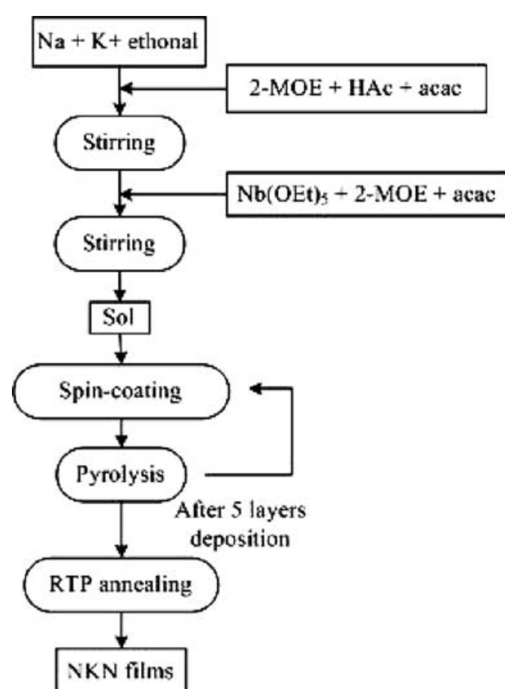

Fig. 1 Procedure for preparing NKN films

5 ml 2-methoxyethanol (abbreviated as 2-MOE) to synthesize sodium ethoxide [$NaOC_2H_5$] and potassium ethoxide [KOC_2H_5]. 2 ml acetic acid (abbreviated as HOAc) and 1 ml acetylacetone (abbreviated as acac) were added as chelating agents so that the alkoxides were stabilized. The mixture at a stoichiometric ratio was stirred and heated at 120°C for 4 h to stabilize the double metal alkoxides. Then stoichiometric amount of niobium pentaethoxide [$Nb(OC_2H_5)_5$] (abbreviated as $Nb(OEt)_5$) dissolved in 5 ml 2-MOE was added. The final mole ratio of 2-MOE to HOAc is about 5. The resultant mixture was kept stirring for another hour and was distilled to reach a final Nb concentration of 0.4 M. All these operations were carried out in air at room temperature. A zirconium-containing organic solution was prepared for the ZrO_2 buffer layer using a similar procedure. We also dissolved 0.001 mol zirconium *n*-propoxide [$Zr(OCH(CH_3)_2)_4$] in 18 ml 2-MOE, adding 1 ml of HOAc and 1 ml of acac to form the solution. The mixture was stirred for 2 h. The concentration was adjusted to 0.05 M solution.

NKN films were deposited onto 10×10 mm^2 Si (100) wafers using a conventional spin-coating method. First, the substrate was spin-coated with a zirconium organic solution, and the gel film was annealed at 500°C for 1 min to form an amorphous ZrO_2 layer which can prevent the diffusion of Si atoms from the substrate into the film. Then the NKN precursor solution was deposited onto the ZrO_2 buffer layer by spin-coating in ambient atmosphere at 3000 rpm for 30 s. After deposition of each layer, the precursor films were naturally dried and pyrolyzed for 3 min to remove organics. The pyrolysis temperature was varied from 200 to 500°C to investigate its effect on the film structure. The spin-coating and pyrolysis treatments were repeated five times to achieve a total thickness of about 0.5 μm. The pyrolyzed films were then annealed at various temperatures from 700 to 900°C for 1 min in a rapid thermal processing (RTP) furnace (RTP-500, Beijing East Star Research Office of Applied Physics, Beijing, China) to form perovskite structure in the films. During the whole annealing processing, it took 20 s to rise from room temperature to 200°C and 10 s to rise from 200°C to the predetermined annealing temperatures. Consequently, the corresponding heating rates for the annealing at 700, 800, 820, 830, 850 and 900°C were 70, 80, 82, 83, 85 and 90°C/s, respectively.

To measure the ferroelectric properties, 100-nm-thick Au electrodes were deposited on the surfaces of the NKN films by sputtering through a mask with an interdigitated strip configuration. The interdigitated electrode was 5 mm in length and 0.5 mm in width with a spacing of 0.5 mm. Electric field was applied in the in-plane direction when the ferroelectric properties are evaluated. The polarization hysteresis loops of the NKN films were evaluated using a ferroelectric tester (TF, axiACCT Analyzer 2000 FE).

TGA analysis of the NKN dried gel sample was conducted using TGA 2050 (TA, USA) with a heating rate of 20°C/min from room temperature to 900°C. The crystallographic structure of the NKN films was examined by X-ray diffraction (XRD, Rigaku, D/max-RB) using Cu-K_α radiation at a scan rate of 3°/min. The surface morphology was observed using a field-emission scanning electron microscope (FE-SEM, JSM-6301F) and an atomic force microscope (AFM, Seiko, SPA-300HV). The cross-sectional microstructure of the films was also inspected by SEM.

3 Results and discussion

3.1 Crystalline phase change and microstructure evolution of NKN films

A homogeneous and stable NKN precursor solution was successively synthesized from potassium ethoxide, sodium ethoxide and niobium pentaethoxide in 2-MOE, which guaranteed the validity of spin-coating technique. To determine the appropriate annealing conditions, Thermogravimetric analysis (TGA) curves and their differential curves were obtained on a dried gel sample, which was obtained from a 0.5 M NKN solution prepared more than one year before by naturally drying. The measurement was conducted in air ambience. The weight of the sample is 8.7930 mg. The result is shown in Fig. 2, which indicated that most of the organics and other volatiles were removed at temperatures below 630°C and the residual materials may be the mixture of oxides corresponding to the metal el-

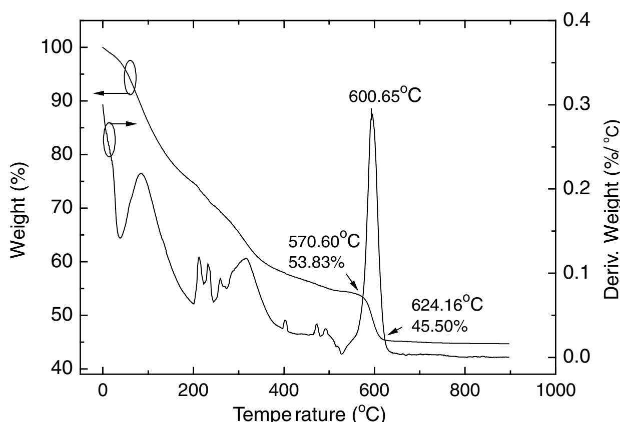

Fig. 2 TGA curves and their differential curves of the $Na_{0.5}K_{0.5}NbO_3$ dried gel heated in air at 20°C/min

ements. Therefore, the annealing experiments were conducted above 630°C for the crystallization process of the films.

To determine the optimal annealing temperature, pyrolyzed multilayer films were annealed at a temperature from 700 to 900°C. The XRD analysis of deposited films with different annealing temperatures revealed that the crystallization of the amorphous (pyrolyzed) films appeared with a small amount of perovskite formation at 800°C, below which there were no perovskite peaks. Figure 3 shows the XRD patterns of the NKN films annealed from 800–900°C for 60 s. All the deposited NKN films were crystallized after annealing, according to the diffraction peaks of the standard powder samples of $NaNbO_3$ (PDF #33-1270) and $KNbO_3$ (PDF #32-0822). The crystallites of the resultant NKN films were randomly oriented. The intensity of the NKN peaks increased with increasing annealing temperature, especially those for the (001) and (011) diffractions at

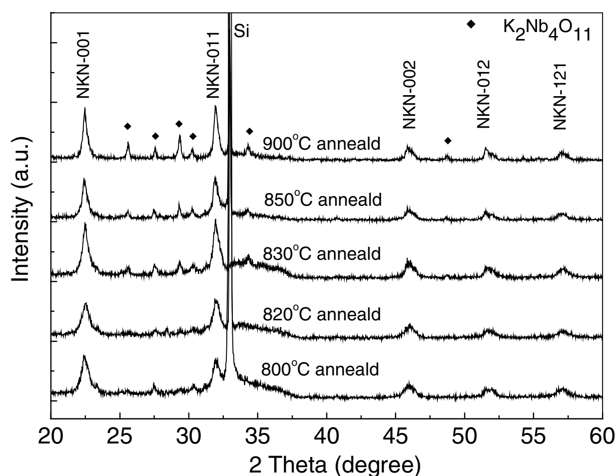

Fig. 3 X-ray diffraction patterns of NKN films deposited 5 times on Si(100) substrates, pyrolyzed at 400°C for 3 min, and annealed at different temperatures for 1 min

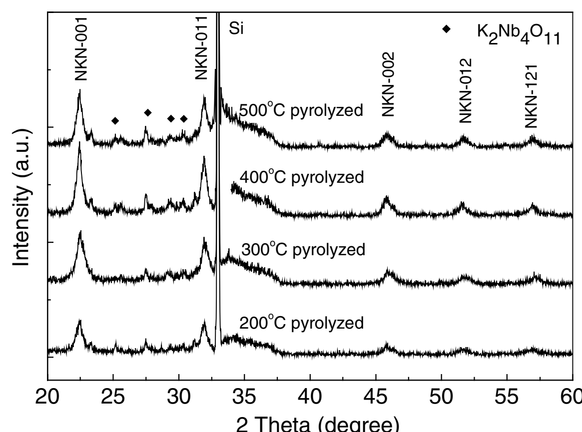

Fig. 4 X-ray diffraction patterns of NKN films deposited 5 times on Si(100) substrates, pyrolyzed at different temperatures for 3 min, and annealed at 800°C for 1 min

~22.3° and ~31.8°, respectively. Miller indices of the NKN perovskite peaks were assigned according to those PLD deposited NKN films reported by Cho et al. [17]. The peaks also became narrower with increasing temperature, indicating crystallite growth and/or improved crystallization. The full width at half-maximum (FWHM) of the NKN(001) reflection changed from 0.66° to 0.30° when the annealing temperature increased from 800 to 900°C. So 830°C is set to be the optimum annealing temperature to ensure both better crystalline quality and less impure phase formation. Several non-perovskite peaks were observed between 25° and 33°, and these peaks may be assigned to a secondary phase, such as $K_2Nb_4O_{11}$. The peak intensity of the $K_2Nb_4O_{11}$ phase also increased at higher annealing temperatures. This is a compound devoid of potassium compared to $KNbO_3$, so one possible reason for the formation of this secondary phase is the volatilization of K component. No obvious peaks of ZrO_2 buffer layer were observed in the XRD patterns probably due to its small thickness.

To get high-quality films fabricated by sol-gel method, pyrolysis condition is very important. The pyrolysis temperature in chemical solution deposition is a very important factor, as the properties of films such as crystallinity and surface morphology can be deeply affected by the volatilization mode of organic compounds during pyrolysis [18, 19]. Furthermore, Gong et al. have found that the pyrolysis temperature has significant effects on the quality of sol-gel derived thin films and different pyrolysis temperatures may cause different orientation growth of thin films [20]. As shown in Fig. 4, the XRD characterization of films prepared with different pyrolysis temperatures shows that the NKN peak intensities varied with the pyrolysis temperature. Weak perovskite peaks can be observed in the XRD patterns of NKN films pyrolyzed at a low temperature (200°C) and annealed at 800°C. When the pyrolysis temperature was 400°C, the

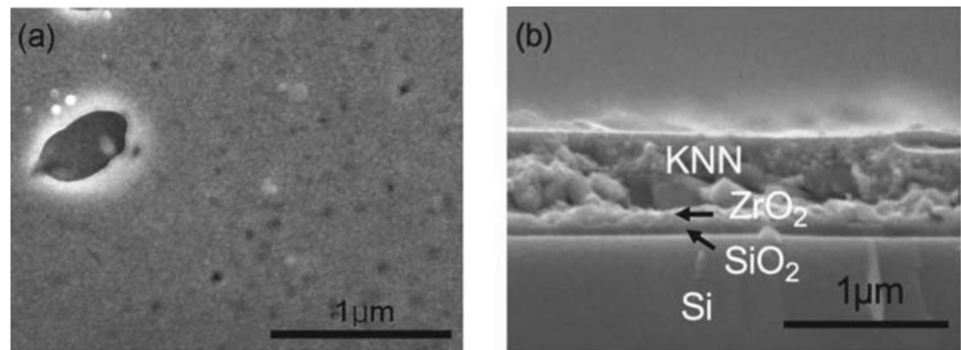

Fig. 5 SEM micrographs of the NKN films deposited on Si(100) substrates, pyrolyzed at 400°C and annealed at 800°C. (a) Surface and (b) cross-section

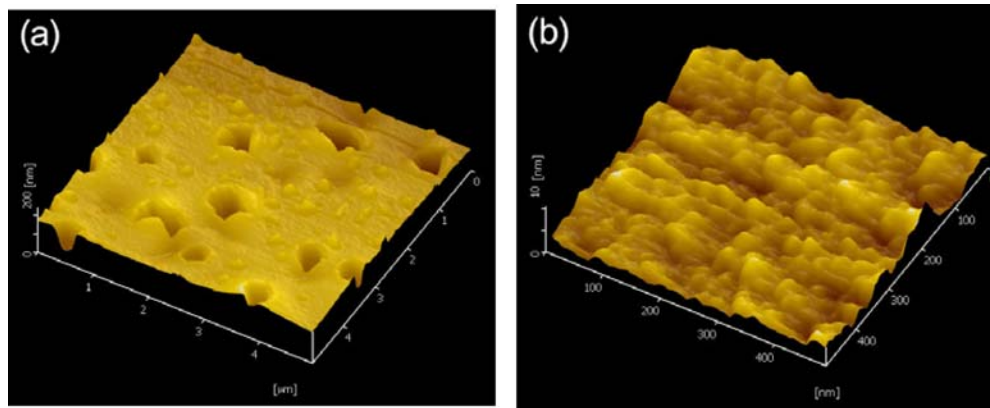

Fig. 6 AFM micrographs of the NKN films deposited on Si(100) substrates, pyrolyzed at 400°C and annealed at 800°C. (a) 5μm × 5μm and (b) 500 nm × 500 nm

NKN film had the narrowest peaks with the highest intensity. Therefore, we set the optimum pyrolysis temperature at 400°C.

SEM morphologies of the representative surface and cross-sectional microstructure of the NKN films show that the present NKN films on Si substrates had relatively dense and uniform microstructure without any cracks and peeling-off (Fig. 5). The sample was pyrolyzed at 400°C and annealed at 800°C through rapid thermal process, which was fairly dense except for some surface pores and particles on their surfaces. The pores may result from the volatilization of organic materials or even Na and K component. As seen in Fig. 5(b), the thickness of 5-layer NKN films was about 500 nm, from which one single layer film was estimated to be 100 nm thick. No distinct interfaces were observed between the five deposited layers of the NKN films.

As shown in AFM images in Fig. 6, at lower magnification (Fig. 6(a)), the pores on the surface were about 80 nm deep, much smaller than the whole thickness of the films. The diameter of the pores varied from 0.3 to 1 μm. At higher magnification, the surface was dense with fine grains of about 50 nm in diameter (Fig. 6(b)). More studies are in progress to explore the optimal pyrolysis and annealing conditions to eliminate the surface defects.

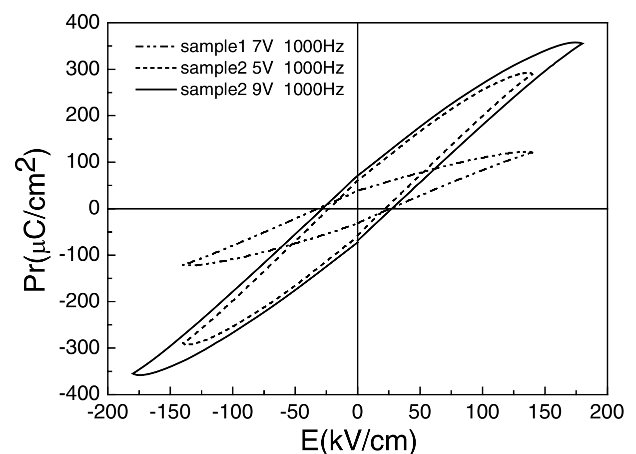

Fig. 7 The P-E curves of the NKN films pyrolyzed at 400°C and annealed at 900°C (sample 1) and 830°C (sample 2) on Si (100) substrates

3.2 Electrical properties of NKN films

The compound $Na_{0.5}K_{0.5}NbO_3$ (NKN) has been considered a good alternative of Pb(Zr, Ti)O_3-based materials for its high Curie temperature T_c, large piezoelectric longitudinal response d_{33} and high planar coupling coefficient K_p. Many researches were conducted to investigate the dielectric or

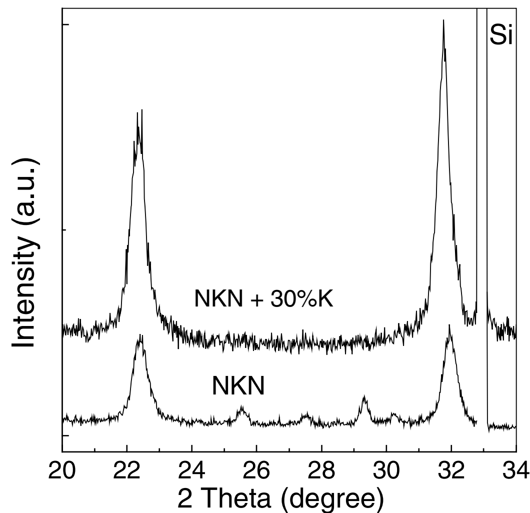

Fig. 8 X-ray diffraction patterns of 5 layer NKN films with and without K compensation. The films were deposited on Si(100) substrates, pyrolyzed at 400°C for 3 min, and annealed at 800°C for 60 s

electrooptic properties of $Na_{0.5}K_{0.5}NbO_3$ film samples [21, 22], or the ferroelectricity of $Na_{0.5}K_{0.5}NbO_3$-based thin films prepared by other methods [23], but there is yet no report about the relative ferroelectric or piezoelectric properties of sol-gel derived NKN films so far [15]. So the characterization of the ferroelectricity and piezoelectricity of NKN films is very meaningful. Figure 7 illustrates the P-E curves of the NKN films prepared in the present study using the sol-gel method, for which the test signals were triangular waves with a frequency of 1000 Hz. Samples 1 and 2 were both 5-layer films pyrolyzed at 400°C, but were annealed at 900°C and 830°C, respectively. For sample 1, the coercive filed was 25.2 kV/cm, which is comparable with those of *c*-axis oriented NKN films, while the remnant polarization in the P-E hysteresis loops was about 38.7 $\mu C/cm^2$ under an electric field of 140 kV/cm, which is a little higher than the reported value of NKN films [17, 24]. For sample 2, the remnant polarization was even higher, reaching 70.2 $\mu C/cm^2$. Although the present result on the measurement of P-E hysteresis loops confirmed the ferroelectricity of the perovskite NKN films, it is considered that the coarse interdigitated (IDT) electrode configuration structures might cause the decrease of the reliability of the above measured values of remnant polarization. Nevertheless, the polarization decreases greatly with increasing annealing temperature as shown in Fig. 7, which is considered to be due to the following reasons. First, increasing the annealing temperature from 830 to 900°C produced more non-perovskite phase $K_2Nb_4O_{11}$ in the film as shown in Fig. 3. Second, the grain growth due to the increase in annealing temperature might weaken the effect of non-ferroelectric phases on the measured polarization, probably due to space charge polarization in grain boundaries.

3.3 Compensation of volatile components

The volatilization of Na and K components in NKN or NKN-based ceramics has great effects on the stoichiometry of the final fabricated materials. Many attempts have been made to avoid the appearance of a secondary phase or to control the stoichiometry of the ceramics by adding an excess amount of alkali metal component [25, 26]. The K/Nb ratio in the impure phase $K_2Nb_4O_{11}$ is 0.5, which is smaller than the value in $KNbO_3$. So 30% excess KOC_2H_5 was added from

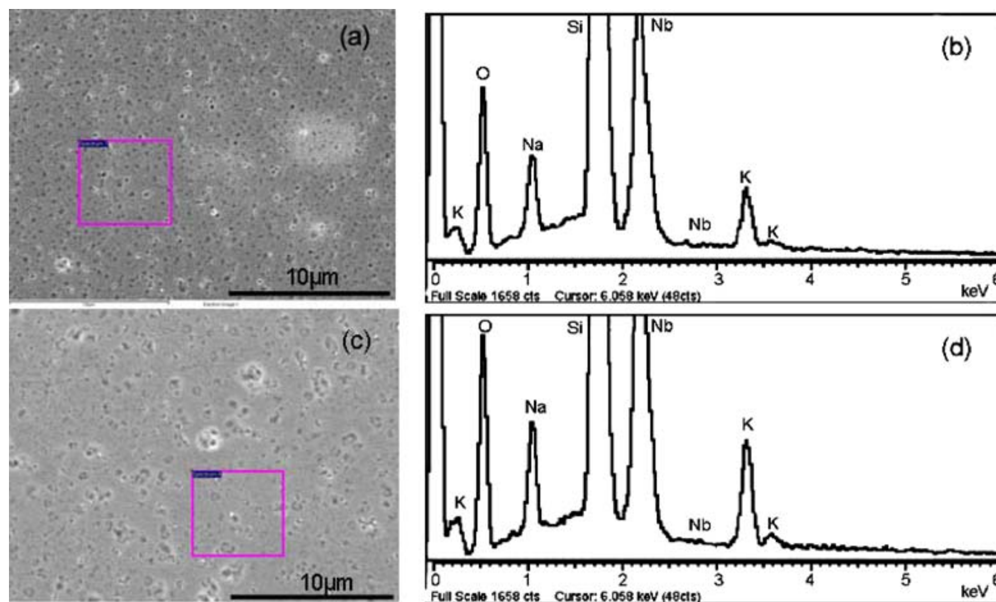

Fig. 9 EDS analysis of 5 layer NKN films (a) with and (b) without K compensation. The films were deposited on Si(100) substrates, pyrolyzed at 400°C for 3 min, and annealed at 800°C for 60 s

Table 1 Chemical compositions of NKN films

Composition	Na/(Na+K)	(Na+K)/Nb
$Na_{0.5}K_{0.5}NbO_3$	0.55	0.67
$Na_{0.5}K_{0.5}NbO_3$+30%K	0.49	0.82

the beginning of the experimental procedure to investigate the effect of compensation of volatile component to the composition of the prepared films.

Figure 8 shows the XRD patterns of NKN films with and without K compensation under the same heat treatment conditions. The peaks of $K_2Nb_4O_{11}$ totally disappear with an increasing intensity of perovskite NKN peaks. As a result, nearly single-phase NKN film was obtained even at the lowest annealing temperature (800°C) used in this work.

Figure 9 shows the EDS analysis images of the NKN films without and with K compensation under the same heat treatment. The distinct increased contents of both Na and K components were observed. The EDS results are listed in Table 1. The ratio of Na/(K+Na) in films without K compensation is a little higher than 0.5, indicating that the volatilization of K is greater than Na. With K compensation, the obtained Na/(K+Na) ratios of the NKN films was near 0.5, and the total ratio of (Na+K)/Nb increased a lot from 0.67 to 0.82. However, Na and K might be evaporated when the samples were irradiated with an electron beam in the EDS measurement. The real ratio of (Na+K)/Nb may be a little higher than the measured value. All these facts suggest that the compensation of volatile components can help control the stoichiometry of the deposited films and can improve the film qualities. Further investigation is needed to find the optimum excess amount of K for the compensation to achieve the best electrical performance.

4 Conclusions

(Na,K)NbO_3 (NKN) thin films deposited on Si (100) substrates with a ZrO_2 buffer layer were successfully prepared by sol-gel processing. The optimum pyrolysis and annealing temperatures were 400°C and about 830°C, respectively. 0.5-μm-thick NKN films with fine grain size of about 50 nm had relatively dense and uniform microstructure without any cracks and peeling-off. The *P*-*E* hysteresis loops proved the ferroelectricity of the NKN films and the remnant polarization was about 38.7 $\mu C/cm^2$. An attempt of compensation of volatile components has been made to improve the quality of the deposited films.

Acknowledgments This work was supported by National Natural Science Foundation of China (Grants Nos. 50325207, 50621201, and 50672040) and the Ministry of Science and Technology of China under the Grant 2002CB613306.

References

1. Singh K, Lingwal V, Bhatt SC, Panwar NS, Semwal BS (2001) Mater Res Bull 36(13–14):2365
2. Ringgarrd E, Wurlitzer T (2005) J Eur Ceram Soc 25:2701
3. Li J-F, Wang K, Zhang B-P, Zhang L-M (2006) J Am Ceram Soc 89(2):706
4. Zhang B-P, Li J-F, Wang K, Zhang HL (2006) J Am Ceram Soc 89(5):1605
5. Lingwal V, Semwal BS, Panwar NS (2003) B Mater Sci 26(6):619
6. Matsubara M, Kikuta K, Hirano S (2005) J Appl Phys 97(11):114105
7. Saito Y, Takao H, Tani T, Nonoyama T, Takatori K, Homma T, Nagaya T, Nakamura M (2004) Nature 432:84
8. Wang X, Helmersson U, Olafsson S, Rudner S, Wernlund LD, Gevorgian S (1998) Appl Phys Lett 73(7):927
9. Gross SJ, Tadigadapa S, Jackson TN, Trolier-McKinstry S, Zhang QQ (2003) Appl Phys Lett 83(1):174
10. Gong W, Li J-F, Peng C-E, Gui ZL, Li LT (2005) Adv Mater 17(16):1952
11. Gong W, Li J-F, Chu XC, Gui ZL, Li LT (2004) J Appl Phys 96(1):590
12. Cho C-R, Koh J-H, Grishin A, Abadei S, Gevorgian S (2000) Appl Phys Lett 76(13):1761
13. Saito T, Wada T, Adachi H, Kanno I (2004) Jpn J Appl Phys 43(9B):6627
14. Cho C-R (2002) Mater Lett 57(4):781
15. Soderlind F, Kall P-O, Helmersson U (2005) J Cryst Growth 281:468
16. Gong W, Li J-F, Chu XC, Lun GZ, Li LT (2004) Appl Phys Lett 85(17):3818
17. Cho C-R, Grishin A (2000) J Appl Phys 87(9):4439
18. Kim BH, An JH, Hwang KS, Kang BA, Nishio K, Tsuchiya T (2004) J Kor Phy Soc 44(2):346
19. Hwang KS, Manabe T, Yamaguchi I, Kumagai T, Mizuta S (1997) Jpn J Appl Phys 36:5221
20. Gong W, Li J-F, Chu XC (2004) J Eur Ceram Soc 24(10–11):2977
21. Kugler VM, Soderlind F, Music D, Helmersson U, Andreasson J, Lindback T (2004) J Cryst Growth 262(1–4):322
22. Bolmqvist M, Khartsev S, Grishin A (2005) IEEE Photonic Tech L 17(8):1638
23. Saito T, Adachi H, Wada T (2004) Jpn J Appl Phys 44(19):L573
24. Bolmqvist M, Koh J-H, Khartsev S, Grishin A (2002) Appl Phys Lett 81(2):337
25. Romanov MV, Korsakov IE, Kaul AR, Stefanvich SY, Bolshakov IA, Wahl G (2004) Chem Vapor Depos 10(6):318
26. Lu T, Chen XM, Jin DZ, Hu X (2005) Mater Res Bull 40(10):1847